

Supporting Information

A Facile Strategy to Fabricate a Skin-like Hydrogel with Adhesive and Highly Stretchable Attributes through Small Molecule Triggering toward Flexible Electronics

Qi Chen^{a, ‡}, Xiang Ke^{a, ‡}, Yusong Cai^a, Hao Wang^a, Zhiyun Dong^a, Xinlong Li^a, Jinlin Li^a, Xinyuan Xu^a, Jun Luo^{a*}, and Jianshu Li^{a,b*}

^aCollege of Polymer Science and Engineering, State Key Laboratory of Polymer Materials Engineering, Sichuan University, Chengdu 610065, P.R. China.

^bState Key Laboratory of Oral Diseases, West China Hospital of Stomatology, Sichuan University, Chengdu 610041, China.

Correspondence: Jun Luo (luojuncd@scu.edu.cn) and Jianshu Li (jianshu_li@scu.edu.cn)

[‡]These authors contributed equally to this work.

Table S1. Composition of hydrogels with different tris content.

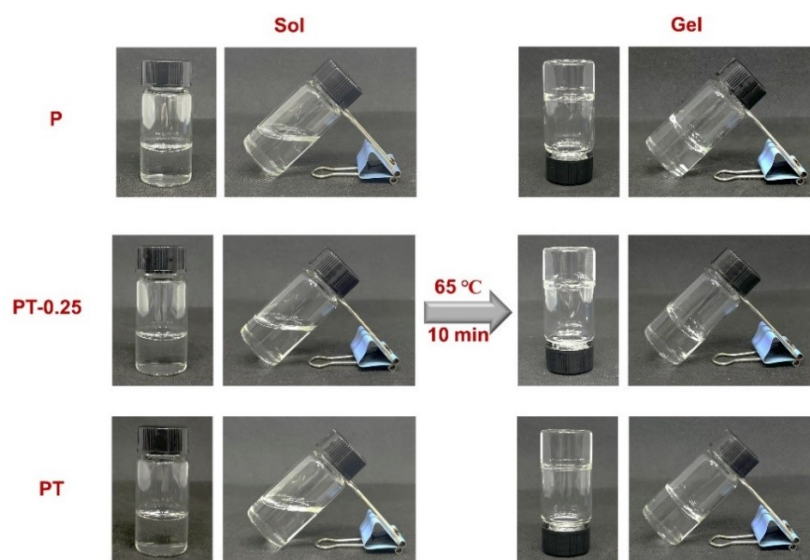
	30 wt% AM (g)	MBA (mg)	APS (mg)	Tris (wt%)	Tris (g)
P				0.00	0.00
PT-0.25	8.00	4.00	8.00	25.00	2.00
PT				50.00	4.00

Table S2. Composition of hydrogels with different tris contents and the pH value of the solution before polymerization.

	30 wt% AM (g)	MBA (mg)	APS (mg)	Tris (wt%)	Tris (g)	pH
P				0.00	0.00	7.23
PT-0.25	8.00	4.00	8.00	25.00	2.00	11.11
PT				50.00	4.00	11.29

Table S3. Composition of hydrogels with different CaCl₂ content.

	30 wt% AM (g)	MBA (mg)	APS (mg)	Tris (g)	CaCl ₂ (wt%)	CaCl ₂ (g)
PT					0.00	0.00
PTC-10%	8.00	4.00	8.00	4.00	10.00	0.80
PTC					30.00	2.40

**Figure S1.** The synthesis process of hydrogels with different tris content.

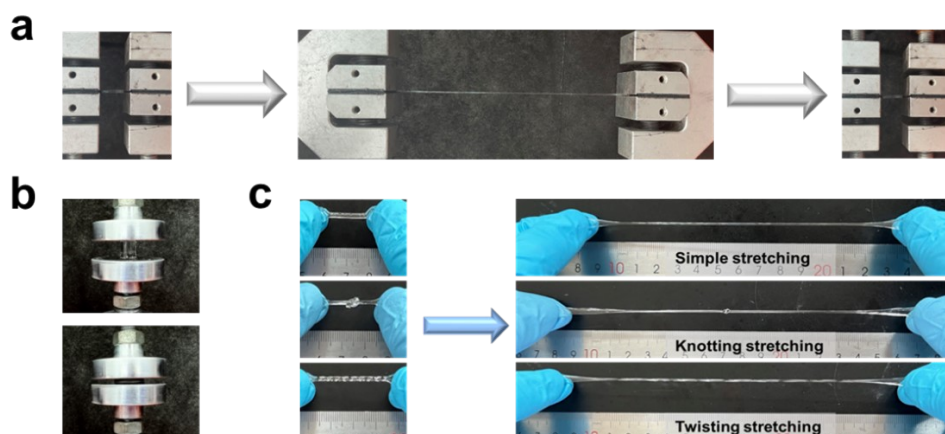


Figure S2. (a-b) Photographs of the PT hydrogel bearing large tension and compression strain; (c) the simple stretching, knotting stretching and twisting stretching.

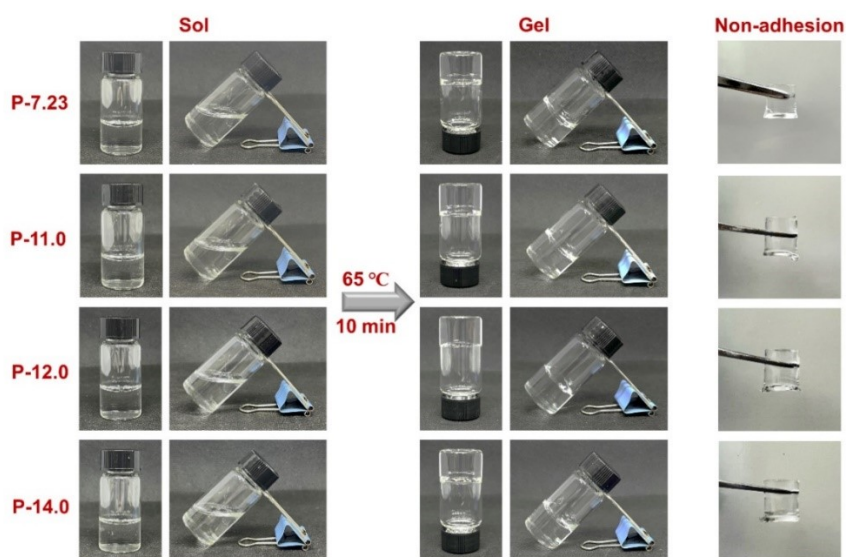


Figure S3. Synthesis process and adhesion of polyacrylamide hydrogels with different pH value adjusted by NaOH.

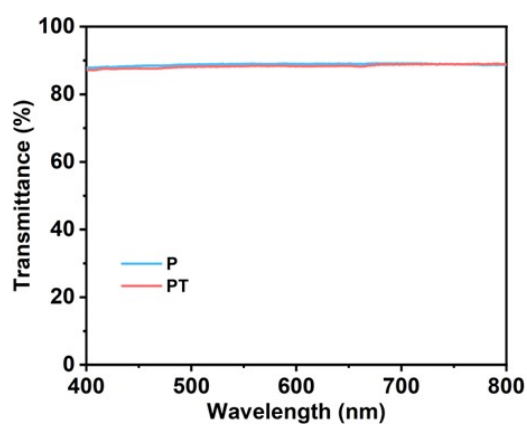


Figure S4. Transmittance of P and PT hydrogels within the visible light spectrum, spanning the range of 400 to 800 nm.

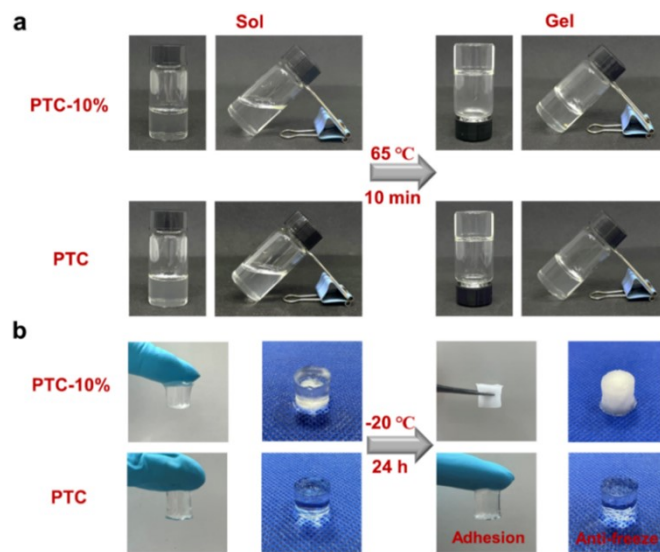


Figure S5. (a) The synthesis process and (b) anti-freezing ability of hydrogels with different CaCl_2 content.

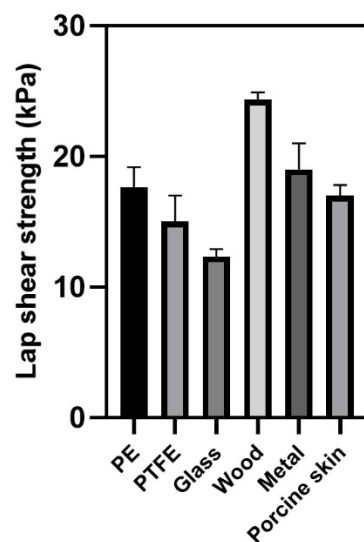


Figure S6. The lap shear strength of PTC hydrogels.

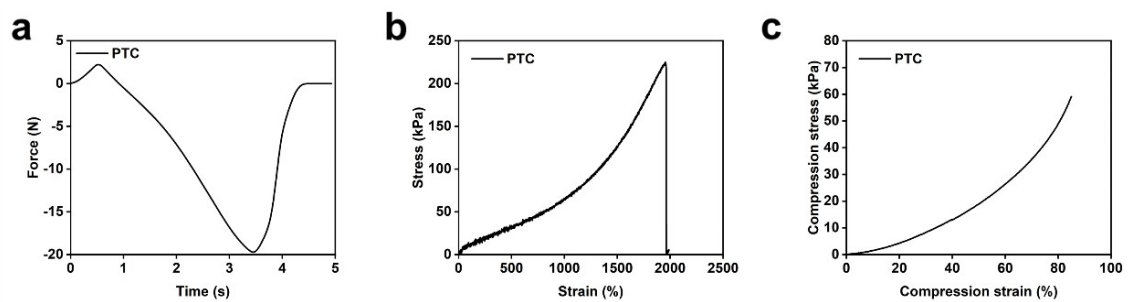


Figure S7. (a) The adhesion force of P, PT and PTC hydrogels; (b) typical uniaxial tensile stress–strain curves and (c) compression stress–strain curves of P, PT and PTC hydrogels.

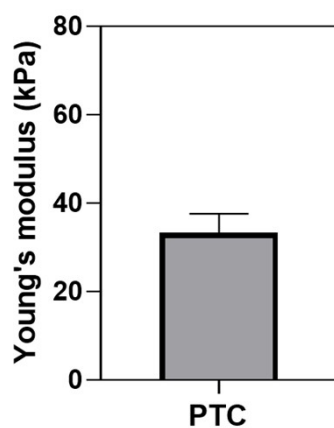


Figure S8. Young's modulus of different hydrogels.

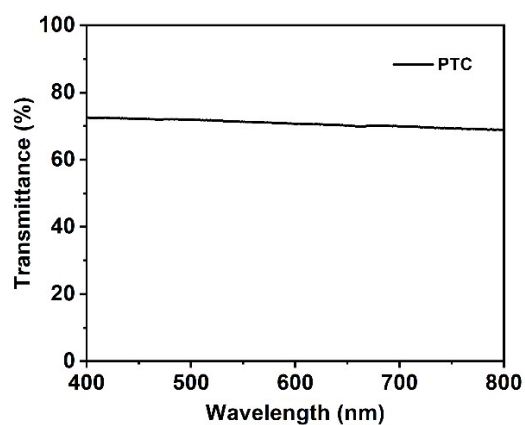


Figure S9. Transmittance of PTC hydrogels within the visible light spectrum, spanning the range of 400 to 800 nm.

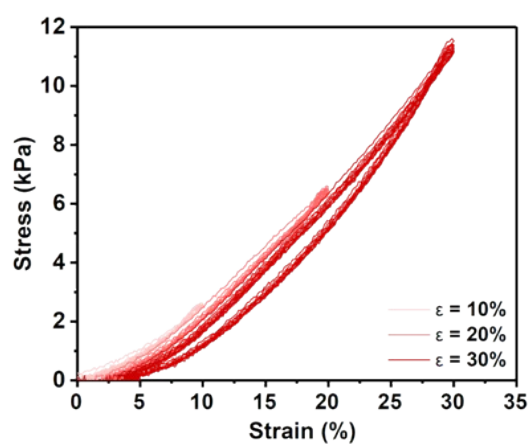


Figure S10. Cyclic compression stress of PTC hydrogel at different strains.

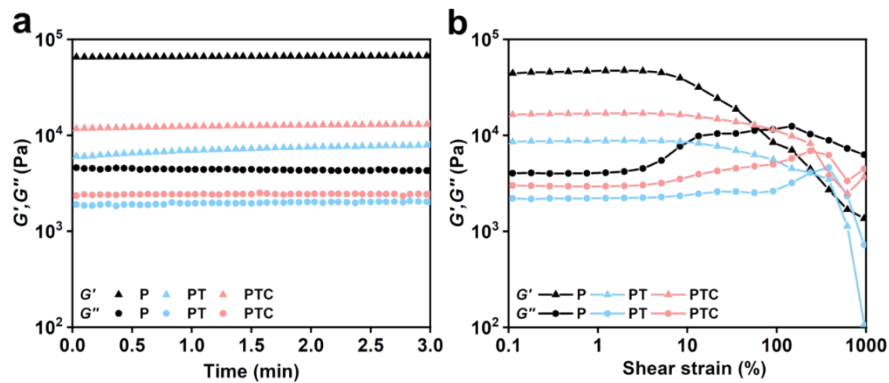


Figure S11. Rheological (a) time sweeps and (b) strain sweeps conducted on P, PT and PTC hydrogels.

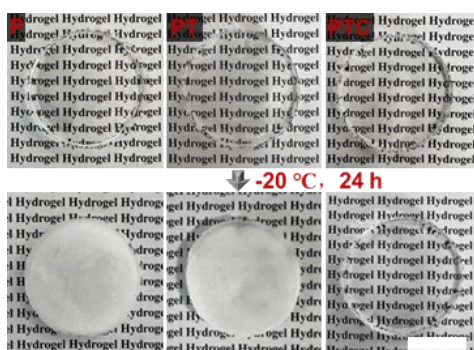


Figure S12. Photographs of P, PT and PTC hydrogels before and after being stored at $-20\text{ }^{\circ}\text{C}$.

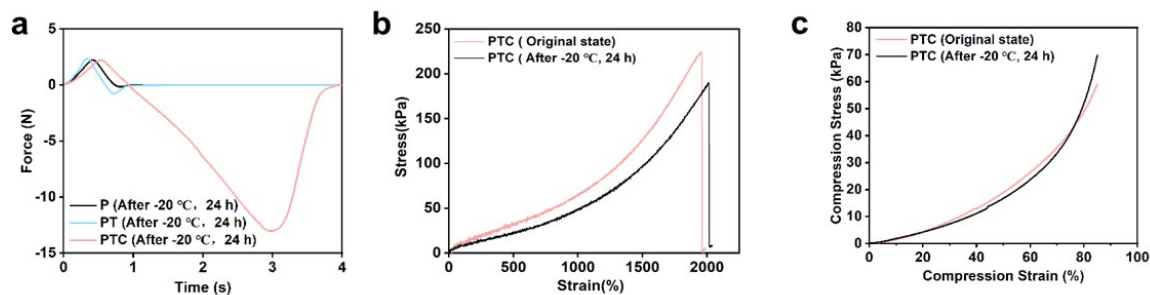


Figure S13. (a) The adhesion force of P, PT, and PTC hydrogels after being frozen for 24 h at $-20\text{ }^{\circ}\text{C}$; (b-c) the tensile and compression properties of PTC hydrogels before and after freezing.

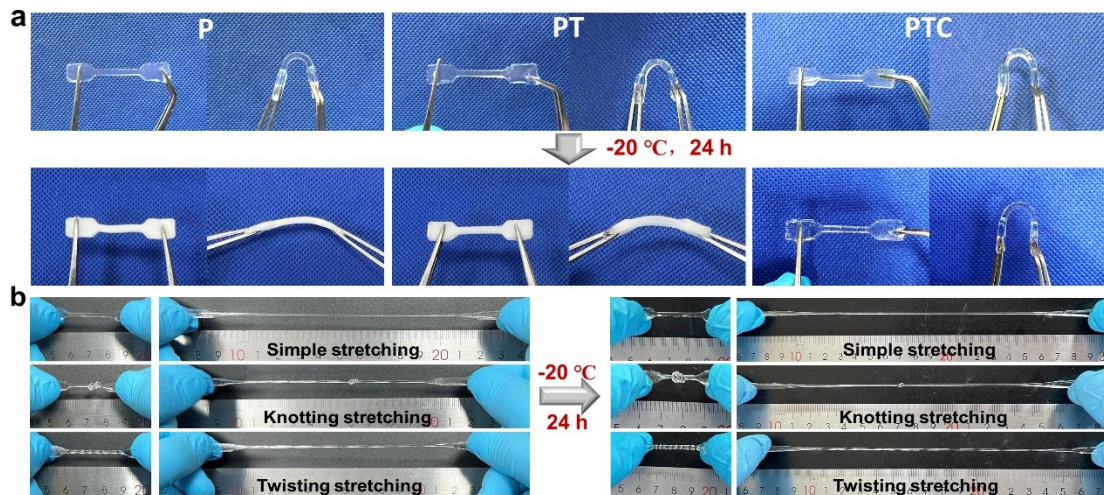


Figure S14. (a) Photographs of P, PT, and PTC hydrogels after being frozen for 24 hours at -20 °C; (b) the tensile properties of PTC hydrogel before and after freezing.

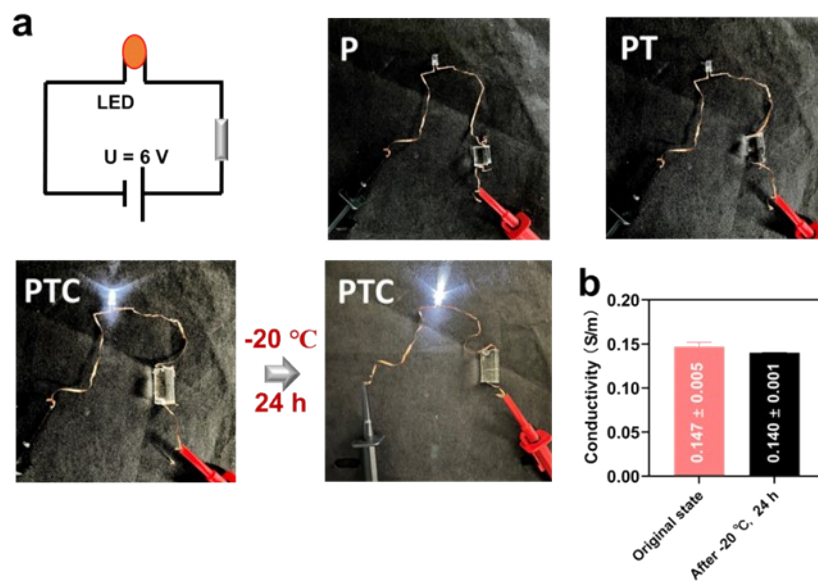


Figure S15. (a) Photographs of the conductive PTC hydrogel that makes LED bright; (b) changes in the electrical conductivity of the PTC hydrogel before and after freezing.

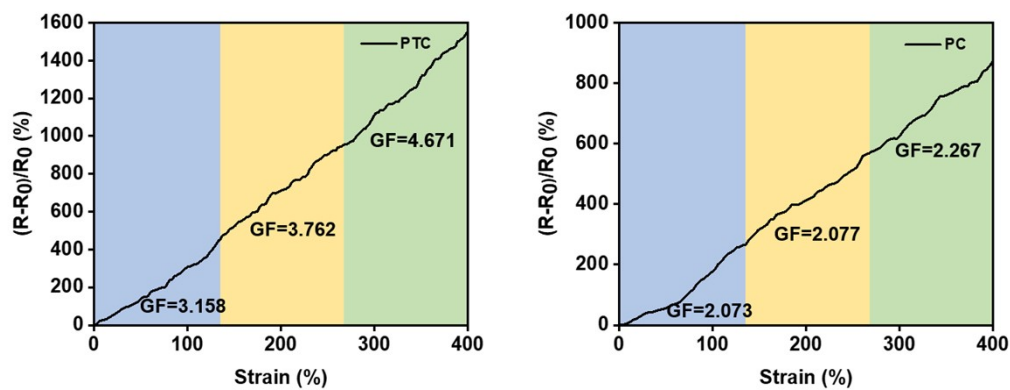


Figure S16. The Gauge factor of PTC and PC hydrogels.

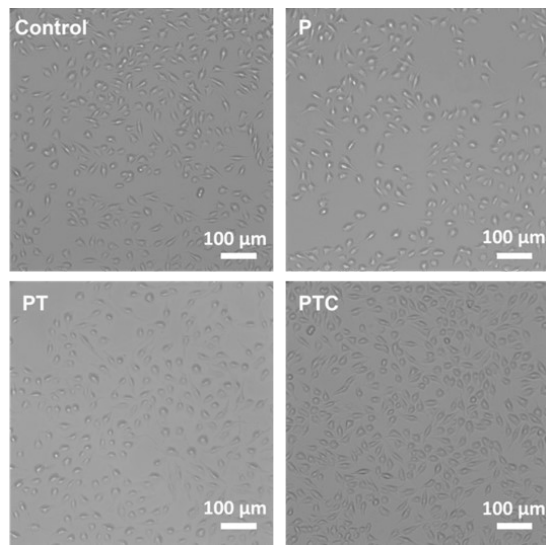


Figure S17. L929 cells morphology after incubation with different hydrogels.